NONSTATIONARY TURBULENT BOUNDARY LAYERS IN INITIAL PIPE LENGTH

A. I. Leont'ev and A. V. Fafurin

UDC 532.526.4

The results are given of an investigation on the effect of flow instability on friction and heat transfer laws as well as the integral characteristics of the boundary layer.

The analysis is based on approximations of tangential stresses and heat fluxes using the method described in [1].

A method is proposed for calculating friction and heat transfer in axially symmetric conduits in the case of nonstationary conditions.

A survey was given in [2] of the present state of research on nonstationary friction and heat transfer. It was shown that solutions are either constructed by using the laws of friction and heat transfer obtained under stationary conditions or criteria are introduced into these laws which take into account the fact that the process is unsteady.

In principle, all solutions refer to laminar flows around surfaces of simple forms.

As a rule, turbulent flows are analyzed by employing the quasistationary approximation which in a number of cases leads to contradictory results. It is our aim in this work to establish laws of friction and heat transfer in the non-stationary case and to develop a computation method under these conditions for the turbulent boundary layer in the initial length of pipe.

1. Laws of Turbulent Friction and Heat Transfer. By its very nature turbulent flow of fluid is not stationary. The time-averaged parameters of turbulent flow are usually given by the formula

$$\bar{u} = \frac{1}{T}\int_0^\tau u(T+t)\,dt,$$

where T is the time during which the averaging takes place. This period should be sufficiently long compared with the time scale of turbulence and sufficiently short compared with the period of any small flow alterations not directly related to turbulence.

If these flow conditions are satisfied it can be assumed that the nonstationarity of the averaged turbulent flow has no direct effect on the structure of the turbulent boundary layer. The preconditions of semiempirical theories of turbulence remain valid for this quasistationary turbulent boundary layer. The Prandtl formula for the turbulent tangential tension

$$\tau_T = \rho\left(l\cdot\frac{\partial \bar{w}_x}{\partial y}\right)^2 \tag{1.1}$$

together with

$$\frac{c_f}{2} = \frac{\tau_w}{\rho_0 \bar{w}_0^2}; \quad l = \varkappa y\sqrt{\bar{\tau}_0} \tag{1.2}$$

results [1] in

Institute of High Temperatures, Academy of Sciences of the USSR, Moscow. Translated from Inzhenerno-Fizicheskii Zhurnal, Vol. 25, No. 3, pp. 389-402, September, 1973. Original article submitted December 20, 1972.

$$\left(\frac{c_f}{c_{f0}}\right)_{R^{++}} = \left\{\frac{\int_{\omega_1}^{1}\sqrt{\frac{\rho}{\rho_0}}\,d\omega}{\sqrt{\frac{c_{f0}}{2}}\int_{\xi_1}^{1}\sqrt{\frac{\bar{\tau}}{\bar{\tau}_0}}\cdot\frac{d\xi}{\varkappa\xi}}\right\}^2; \quad \xi = \frac{y}{\delta}. \tag{1.3}$$

All notations and subscripts are taken from [1].

The formula (1.3) can be integrated provided the distribution is known of the tangential tensions across the boundary layer. An approximating polynomial proposed in [1] is used to determine them, namely

$$\bar{\tau} = a + b\xi + c\xi^2 + d\xi^3, \tag{1.4}$$

whose coefficients can be found from the boundary conditions

$$\xi = 1, \quad \bar{\tau} = 0, \quad \frac{\partial\bar{\tau}}{\partial\xi} = 0; \quad \xi = 0, \quad \bar{\tau} = 1, \quad \frac{\partial\bar{\tau}}{\partial\xi} = \left(\frac{\partial\bar{\tau}}{\partial\xi}\right)_w. \tag{1.5}$$

By inserting (1.5) in (1.4) one finds

$$\frac{\bar{\tau}}{\bar{\tau}_0} = 1 + \frac{\xi}{2\xi + 1}\left(\frac{\partial\bar{\tau}}{\partial\xi}\right)_w, \quad \bar{\tau}_0 = 1 + 2\xi^3 - 3\xi^2, \tag{1.6}$$

where $\bar{\tau}_0$ is the distribution of tangential tensions along the thickness of an isothermic boundary layer on a nonpermeable smooth plate.

The value of the derivative at the wall can be found if one writes the equation of motion for the region under consideration. One has

$$-\frac{dP}{dx} + \frac{1}{r}\cdot\frac{\partial}{\partial r}(r\tau) = 0. \tag{1.7}$$

In view of

$$-\frac{dP}{dx} = \rho_0\frac{\partial w_0}{\partial t} + \rho_0 w_0\frac{\partial w_0}{\partial x}, \tag{1.8}$$

one obtains from (1.7)

$$\left(\frac{\partial\bar{\tau}}{\partial\xi}\right)_w = z + \lambda + b_1\frac{\omega}{\xi} - \frac{\delta}{r_0}. \tag{1.9}$$

In the case of a stationary flow z = 0, $r_0 \to \infty$ past a planar plate there follows from (1.9)

$$\left(\frac{\partial\bar{\tau}}{\partial\xi}\right)_w = \lambda + b_1\frac{\omega}{\xi}, \tag{1.10}$$

previously obtained in [1].

The following were adopted in (1.9):

$$z = -\frac{\delta}{\tau_w}\rho_0\frac{\partial w_0}{\partial t}; \quad \lambda = -\frac{\delta}{\tau_w}\rho_0 w_0\frac{\partial w_0}{\partial x}, \qquad b_1 = -\frac{(\rho w)_w}{\rho_0 w_0}\cdot\frac{2}{c_f}. \tag{1.11}$$

By inserting (1.9) in (1.6) it is found that

$$\frac{\bar{\tau}}{\bar{\tau}_0} = 1 + \frac{\xi}{2\xi + 1}\left\{z + \lambda + b_1\frac{\omega}{\xi} - \frac{\delta}{r_0}\right\}. \tag{1.12}$$

By substituting (1.12) in (1.3) and integrating the latter with $b_1 = 0$ and by employing the Reynolds analogy,

$$\omega = \frac{h^* - h_w}{h_w^* - h_w} \tag{1.13}$$

one obtains

$$\Psi_{R^{++}} = \left\{\frac{2(1-\omega_1)}{\left(\sqrt{\psi_h} + (1-\psi_h)\omega_1\right)\frac{1}{x}\sqrt{\frac{c_{f_0}}{2}}F}\right\}, \tag{1.14}$$

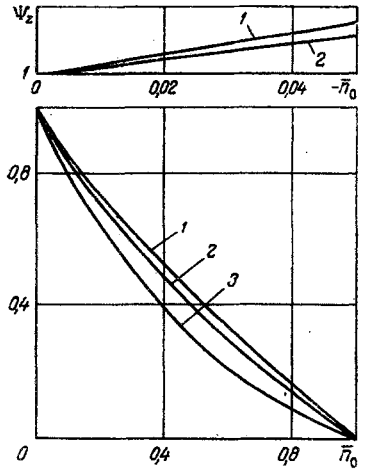

Fig. 1

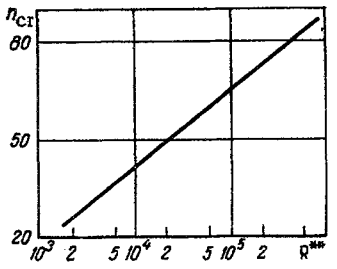

Fig. 2

Fig. 1. Computational results of the relative friction coefficient: curve 1) $R^{++} = 2 \cdot 10$; curve 2) 10; curve 3) 10; $\psi_h = 1$. The lines follow formula (1.14).

Fig. 2. The critical parameter $n_{0\,cr}$ vs R^{++}.

$$\Psi_{R^{++}} = \left(\frac{c_f}{c_{f_0}}\right)_{R^{++}} F = \ln\left|\frac{(\sqrt{3}-\sqrt{1+n})(\sqrt{1+2\xi_1}+\sqrt{1+n\xi_1})}{(\sqrt{3}+\sqrt{1+n})(\sqrt{1+2\xi_1}-\sqrt{1+n\xi_1})}\right| + \sqrt{\frac{n}{2}}\ln\left|\frac{\left(\sqrt{\frac{3}{2}n}+\sqrt{1+n}\right)\left(\sqrt{\frac{n}{2}(1+2\xi_1)}-\sqrt{1-n\xi_1}\right)}{\left(\sqrt{\frac{3}{2}n}-\sqrt{1+n}\right)\left(\sqrt{\frac{n}{2}1+2\xi_1}+\sqrt{1+n\xi_1}\right)}\right|, \tag{1.15}$$

$$n = 2 + z + \lambda - \frac{\delta}{r_0}.$$

The equation of motion for the region of the laminar sublayer can be written as

$$\mu_w \frac{dw_x}{dy} = \tau_w - \left(\rho_0 \frac{\partial w_0}{\partial t} + \rho_0 w_0 \frac{\partial w_0}{\partial x}\right) y + (\rho w)_w w_x. \tag{1.16}$$

By integrating (1.16) between the variability limits of the sought quantities (ξ_1 and w_1) the following expression is obtained for the relative velocity at the boundary of the laminary sublayer

$$\omega_1 = R_w^{++}\frac{\delta}{\delta^{++}}\left\{\frac{c_f}{2}\xi_1 - \frac{\delta}{w_0^2}\cdot\frac{\partial w_0}{\partial t}\cdot\frac{\xi_1^2}{2} - \frac{\delta}{w_0}\cdot\frac{\partial w_0}{\partial x}\cdot\frac{\xi_1^2}{2} + \frac{(\rho w)_w}{\rho_0 w_0}\int_0^{\xi_1}\omega d\xi\right\}. \tag{1.17}$$

One has the identity

$$\frac{\omega_1}{R_w^{++}\delta/\delta^{++}} = \frac{R_0}{\xi_1 (R_w^{++}\delta/\delta^{++})^2}. \tag{1.18}$$

It was shown in [3] that the number R_0 proved a conservative quantity for accelerated and slowed down flows. If one takes it as equal to its value under standard conditions one obtains from (1.17) together with (1.18)

$$\xi_1 = \frac{\sqrt{R_0}}{R^{++}\frac{\delta}{\delta^{++}}\sqrt{\Psi\frac{c_{f_0}}{2}\left(1 + z\frac{\xi_1}{2} + \lambda\frac{\xi_1}{2} + \frac{b_1}{\xi_1}\int_0^{\xi_1}\omega_1 d\xi\right.}}. \tag{1.19}$$

The analysis of Eqs. (1.14), (1.17), and (1.19) shows that for some values of the parameters which determine friction there may occur a case in which the friction coefficient vanishes. From the physical point of view this would indicate that the flow becomes separated from the wall. A similar case occurs when the parameter $n_0 = h\Psi$ becomes equal to its limiting value.

If in stationary flows the separation occurs for the critical values, $\lambda_0 = \lambda_{0cr}$ then in nonstationary flows the separation may take place for any λ_0 and the time-derivative of the velocity must be negative, that is, in the case of a simultaneous effect of nonstationarity and pressure gradient the flow separation is possible in narrowing conduits and its stabilization in widening ones.

The value of the critical parameter n_{0cr} can be found from (1.13) if one assumes that $n_0 \to n_{0cr}$, $\omega_1 \to \omega_{1cr}$, $\xi_1 \to \xi_{1cr}$, $b_1 \to 0$, $c_f \to 0$. One has

$$n_{0cr} = \left\{ \frac{2(1-\omega_{1cr})}{\sqrt{\psi_h + (1-\psi_h)\omega_{1cr}}\,\frac{1}{x}\sqrt{\frac{c_{f_0}}{2}\ln|B|}} \right\}^2, \tag{1.20}$$

$$B = 2\left(\sqrt{\frac{3}{2}}+1\right)^2 \left(\sqrt{1+2\xi_{1cr}} + \sqrt{2\xi_{1cr}}\right)^2, \tag{1.21}$$

$$\omega_{1cr} = R_\omega^{++}\,\frac{\delta}{\delta^{++}}\cdot\frac{c_{f_0}}{2}\,\frac{\xi_{1cr}^2}{2}\,n_{0cr},$$

$$\xi_{1cr} = \sqrt[3]{\frac{R_0}{2\,\frac{(R^{++}\delta/\delta^{++})^2}{\frac{c_{f_0}}{2}n_{0cr}}}}. \tag{1.22}$$

In Fig. 1 computational results are shown of the relative friction coefficient vs factor; in the latter the parameter n_0 under consideration is taken into account normalized by n_{0cr} for different values of the Reynolds number R^{++}. Its decrease is distinctly noticeable with the increase of the parameter n_0. Moreover, one can observe a lamination as regards the number R^{++}. In the region of positive acceleration there is only a small increase in the relative friction coefficient, not exceeding 10%.

In Fig. 2 the critical parameter n_{0cr} is shown as a function of the number R^{++}. The quantity n_{0cr} increases with R^{++} increasing which is due to greater stability of the turbulent boundary layer.

The heat transfer law can be found from the hypothesis that the specific heat flux is proportional to the gradients of velocity and of enthalpy [3],

$$q = \rho\left(l\frac{\partial w_x}{\partial y} - l_h\frac{\partial h^*}{\partial y}\right). \tag{1.23}$$

It was shown in [4] that for Pr ~ 1 one has

$$\bar{l} \sim \bar{l}_h; \quad \frac{\partial\omega}{\partial\xi} \sim \frac{\partial\theta}{\partial\xi}.$$

A two-layer model of the heat boundary layers is adopted [5]. Then transforming (1.23) one obtains a relation for the relative heat transfer coefficient in the form

$$\Psi_{R^{++}} = \left\{ \frac{\int_{\theta_1}^{1}\sqrt{\frac{\rho}{\rho_0}}\,d\theta}{\frac{1}{\varkappa}\sqrt{S}\,t_0\int_{\xi_{1h}}^{1}\sqrt{\frac{\bar{q}}{\bar{q}_0}}\cdot\frac{d\xi}{\xi}} \right\}^2. \tag{1.24}$$

Thus in this case as in the derivation of the friction law the distribution of heat fluxes across the boundary layer must be known. A cubic parabola approximation, similar to (1.14), for the boundary conditions

$$\xi = 1, \quad \bar{q} = 0, \quad \frac{\partial\bar{q}}{\partial\xi} = 0; \quad \xi = 0, \quad \bar{q} = 1, \quad \frac{\partial\bar{q}}{\partial\xi} = \left(\frac{\partial\bar{q}}{\partial\xi}\right)_w \tag{1.25}$$

results in the following relation:

$$\frac{\bar{q}}{\bar{q}_0} = 1 + \frac{\xi}{2\xi+1}\left\{z_h + \frac{b_{1h}\theta}{\xi} - \frac{\delta_h}{r_0}\right\},$$

$$z_h = -\frac{\delta_h}{w_0\,\mathrm{St}}\cdot\frac{1}{1-\psi_h}\cdot\frac{\partial\ln\psi_h}{\partial t} \quad \text{for } 1-\psi_h > 0, \tag{1.26}$$

$$z_h = + \frac{\delta_h}{w_0 \mathrm{St}} \cdot \frac{1}{1-\varphi_h} \cdot \frac{\partial \ln \psi_h}{\partial t} \quad \text{for} \quad 1 - \psi_h < 0, \tag{1.27}$$

$\bar{q}_0$ being the heat-flux distribution by thickness of the quasithermal boundary layer on the impermeable smooth plate.

The parameters on the boundary of the heat laminar sublayer can be found from the following considerations.

The energy equation for the region directly adjoining the wall can be written as follows:

$$\rho_w \frac{\partial (h_w - h_0^*)}{\partial t} + \frac{\rho w_y \partial (h_w - h^*)}{\partial y} = \frac{\mu}{\mathrm{Pr}} \cdot \frac{\partial}{\partial y} (h_w - h^*). \tag{1.28}$$

By integrating (1.28) with respect to the transversal coordinate y one obtains

$$\frac{\mu}{\mathrm{Pr}} \cdot \frac{\partial}{\partial y} (h_w - h^*) = q_w - \rho_w \frac{\partial (h_w - h_0^*)}{\partial t} y + (\rho w)_w (h_w - h^*). \tag{1.29}$$

The dimensionless enthalpy at the boundary of the laminar sublayer is found by integrating (1.29). One has

$$\theta_1 = \mathrm{Pr}\, R_h^{++} \frac{\delta_h}{\delta_h^{++}} \left\{ \mathrm{St}\, \xi_{1h} - \frac{\delta_h}{w_0} \cdot \frac{1}{\psi_h (1-\psi_h)} \cdot \frac{\partial}{\partial t} (1-\psi_h) \times \frac{\xi_{1h}^2}{2} + \frac{(\rho w)_w}{\rho_0 w_0} \int_0^{\xi_{1h}} \theta d\xi \right\}. \tag{1.30}$$

By introducing the stability criterion of the laminar sublayer in (1.30) by means of the relation

$$\frac{\theta_1}{R_h^{++} \left(\frac{\delta}{\delta^{++}} \right)_h} = \frac{\eta_h}{\xi_{1h} \left(R_h^{++} \left| \frac{\delta}{\delta^{++}} \right|_h \right)^2}, \tag{1.31}$$

one obtains

$$\xi_{1h} = \frac{\sqrt{\eta_h}}{R_h^{++} \left(\frac{\delta}{\delta^{++}} \right)_h \sqrt{\mathrm{St} \left(1 + z_h \frac{\xi_{1h}^2}{2} + \frac{b_{1h}}{\xi_{1h}} \int_0^{\xi_{1h}} \theta d\xi \right)}}. \tag{1.32}$$

By solving the simultaneous equations (1.26), (1.27), and (1.24) and integrating the latter for $b_{1h} = 0$ and employing (1.13) one finds

$$\psi_h = \left\{ \frac{2}{\sqrt{\psi_h + (1-\psi_h)\theta_1} + 1} \cdot \frac{1-\theta_1}{1-\theta_{10}} \cdot \frac{-\ln \xi_{10}}{Q_h} \right\}^2, \tag{1.33}$$

where Q_h is determined by (1.15) with $Q_h = F$, $\xi_1 = \xi_{1h}$.

Nonstationary heat transfer is characterized in principle by heating or cooling of the surface. The anisotropy parameter Ψ_h tends therefore asymptotically with $t \to \infty$ to unity, that is, $t \to \infty$, $\psi_h \to 1$; $\partial \psi_h / \partial t \to 0$, having eliminated the indeterminacy it follows from (1.27) that $z_h \to 0$. Then $\theta_1 \to \theta_{10}$; $Q_h \to \ln \xi_{1h}$ and $\psi_h \to 1$. For $z_h = 0$ and $\psi_h \neq 1$ the previously obtained result in [6] follows from (1.33).

Let $R^{++} \to \infty$. Then by removing the indeterminacy in (1.33) it is found that the relative heat-transfer coefficient in the limiting case under consideration is independent of the nonstationarity, that is, $\psi_z = 1$. Equations (1.14), (1.17), (1.19) and (1.30), (1.32) and (1.33) are of such structure that their solution and the numerical results are the same provided one starts with the same data ($R^{++} = R_h^{++}$; $z = z_h$).

Therefore, the computational results obtained by using (1.30), (1.32) and (1.33) can be shown in Fig. 1.

In the case of heating up when ψ_h approaches unity $(1 - \psi_h) > 0$ the derivative is positive and the heat-transfer coefficient exceeds its value in stationary conditions. Physically, this is explained by an additional loss of energy proceeding from the heat carrier to the cool wall so that the enthalpy profile across the boundary layer can be reconstructed. In the case of cooling ψ_h approaches zero. In such a case the relative coefficient of heat transfer is less than unity and the heat-transfer process is less intensive.

2. Profiles of Velocities and Enthalpy and Integral Characteristics. If Eq. (1.3) is integrated between variable limits with respect to w and ξ then the velocity can be found in the turbulent core of the

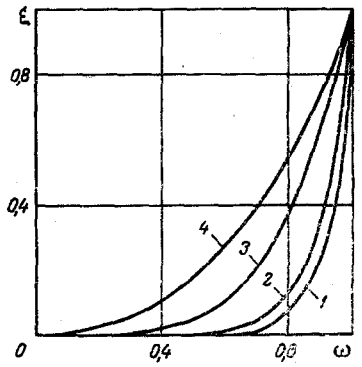

Fig. 3

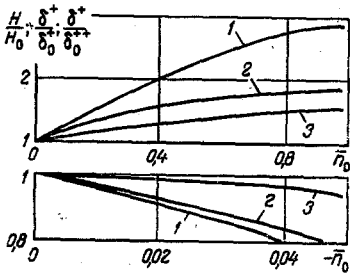

Fig. 4

Fig. 3. Calculation results of the velocity profile: curve 1) $z_0 = -1.99$; curve 2) 0; curve 3) 15; curve 4) $z_{0cr} = 42.5$. Curves — the calculations follow (2.1).

Fig. 4. Integral characteristics of the turbulent boundary layer for $R^{++} = 10^4$: 1) δ^+/δ_0^+; 2) $\delta^{++}/\delta_0^{++}$; 3) H/H_0. Curves — the calculations follow (2.5).

boundary layer as a function of the transversal coordinate by keeping the values of R^{++} and z fixed. By inserting (1.12) into (1.13), integrating the result and finally solving the obtained result for the sought quantity one obtains

$$\omega_i = \frac{2+(1-\psi_h)a_i^2}{2} - \sqrt{\left\{\frac{2+(1-\psi_h)a_i^2}{2}\right\}^2 - (1-\psi_h a_i^2)}, \tag{2.1}$$

$$a_i = \frac{1}{\varkappa}\sqrt{\frac{c_{f_0}}{2}}F_i, \tag{2.2}$$

where F_i are determined by (1.15) if ξ_1 is replaced by the values of ξ_i.

For $\psi_h = 1$ there follows from (2.1) that

$$\omega_i = 1 - \frac{1}{\varkappa}\sqrt{\frac{c_{f_0}}{2}}F_i, \tag{2.3}$$

for $\psi_h = 1$; if $z \to 0$ one has

$$w_i = 1 + \frac{1}{\varkappa}\sqrt{\frac{cf_0}{2}}\ln\xi_i. \tag{2.4}$$

In the case of critical profile the relation can be expressed by the formula (2.1), the quantity a_i being given in this case by

$$a_{i\,cr} = \frac{1}{\varkappa}\sqrt{\frac{c_{f_0}}{2}}\sqrt{\frac{z_{0cr}}{2}}\ln\left|2\left(1+\sqrt{\frac{3}{2}}\right)^2\left(\sqrt{1+2\xi_i}-\sqrt{2\xi_i}\right)^2\right|.$$

In Fig. 3 calculation results are shown of the velocity profile for $R^{++} = 10^4$ and for different values of z_0. It is clear that if the flow is decelerated then the velocity profile is reduced but with acceleration it makes up for it. From the point of view of the reaction of the boundary layer to an external force this can be explained by the formation of another boundary layer and by the associated reconstruction.

By inserting (2.1) in the expressions for displacement thickness and for loss of momenta, namely

$$\frac{\delta^+}{\delta} = \int_0^1\left(1-\frac{\rho}{\rho_0}\omega\right)\left(1-\frac{y}{r_0}\right)d\xi,$$

$$\frac{\delta^{++}}{\delta} = \int_0^1\frac{\rho}{\rho_0}\omega(1-\omega)\left(1-\frac{y}{r_0}\right)d\xi, \tag{2.5}$$

the sought relations can be obtained. In particular, one has for the displacement thickness

$$\frac{\delta^+}{\delta} = \frac{1}{\varkappa}\sqrt{\frac{c_{f_0}}{2}}\left[\frac{1}{2}\sqrt{\frac{n_0}{2}}\left(\frac{2\Psi_z}{n_0}-1\right)\ln\sqrt{\left|\frac{B}{C}\right|} + \frac{1}{2}\sqrt{3(\Psi_z+n_0)}\right.$$

$$-\sqrt{\Psi}/2-\frac{\delta}{r_0}\left\{-\frac{1}{8}\sqrt{\frac{n_0}{2}}\left(\frac{\Psi_z^2}{n_0^2}+\frac{\Psi_z}{n_0}-\frac{3}{4}\right)\ln\sqrt{\left|\frac{B}{C}\right|}\right.$$

$$-\frac{1}{8}\left(\frac{\Psi_z^2}{n_0^2}-3\frac{\Psi_z}{n_0}+\frac{5}{4}\right)\cdot\frac{\sqrt{3(\Psi_z+n_0)}-\sqrt{\Psi_z}}{1-2\frac{\Psi_z}{n_0}}$$

$$\left.+\frac{1}{4}\left(\frac{\Psi_z^2}{n_0^2}-\frac{\Psi_z}{n}+\frac{1}{4}\right)\frac{3\sqrt{3(\Psi_z+n_0)}-\sqrt{\Psi_z}}{\left(1-\frac{2\Psi_z}{n_0}\right)^2}\right\}. \tag{2.6}$$

The following were introduced in (2.6):

$$B=\frac{\sqrt{\frac{3}{2}n_0}+\sqrt{\Psi_z+n_0}}{\sqrt{\frac{3}{2}n_0}-\sqrt{\Psi_z+n_0}},\quad C=\frac{1+\sqrt{\frac{2\Psi_z}{n_0}}}{1-\sqrt{\frac{2\Psi_z}{n_0}}}.$$

In Fig. 4 the integral characteristics of the turbulent boundary layer are shown for $R^{++}=10^4$ as a function of the nonstationarity parameter. One observes that they are essentially different from their values obtained under stationary conditions.

The distribution of enthalpy across the boundary layer can be found from (1.24). Integrating (1.24) between the limits of variation of the sought quantities one obtains

$$\theta=\frac{\left(1-\frac{1-\psi_h}{2}d\right)^2-\psi_h}{1-\psi_h}, \tag{2.7}$$

where

$$d=\frac{\sqrt{St_0}}{x}\Psi_h Q_{hi},$$

$$Q_h=\ln\left|\frac{(\sqrt{3}-\sqrt{1+n_h})(\sqrt{1+2\xi_i}+\sqrt{1-n_h\xi_i})}{(\sqrt{3}+\sqrt{1+n_h})(\sqrt{1+2\xi_i}-\sqrt{1-n_h\xi_i})}\right|$$

$$+\sqrt{\frac{n_h}{2}}\ln\left|\frac{\left(\sqrt{\frac{3}{2}n_h}+\sqrt{1+n_h}\right)\left(\frac{n_h}{2}(1-2\xi_i)-\sqrt{1-n_h\xi_i}\right)}{\left(\sqrt{\frac{3}{2}n_h}-\sqrt{1+n_h}\right)\left(\frac{n_h}{2}(1+2\xi_i)+\sqrt{1+n_h\xi_i}\right)}\right|,$$

$$n_h=2+z_h-\frac{\delta_h}{r_0}.$$

For the flow of an incompressible fluid, (2.7) implies

$$\theta=1-d. \tag{2.8}$$

3. Evolution of Turbulent Boundary Layer in Initial Length of Pipe in a Nonstationarity Case. In the case under consideration it is convenient to write the system of equations in the form

$$\frac{\partial\delta^{++}}{\partial x}+\frac{\delta^{++}}{w_0}\cdot\frac{\partial w_0}{\partial x}(2+H)+\frac{\delta^{++}}{\rho_0}\cdot\frac{\partial\rho_0}{\partial x}=\frac{c_f}{2}-\frac{1}{\rho_0 w_0^2}\cdot\frac{\partial\rho_0 w_0\delta^+}{\partial t}, \tag{3.1}$$

$$\frac{\partial\delta_h^{++}}{\partial x}-\frac{\delta_h^{++}}{w_0}\cdot\frac{\partial w_0}{\partial x}+\frac{\delta_h^{++}}{\rho_0}\cdot\frac{\partial\rho_0}{\partial x}-\frac{\delta_h^{++}}{\Delta h}\cdot\frac{\partial\Delta h}{\partial x}$$

$$=St-\frac{1}{\Delta h w_0}\cdot\frac{\partial\Delta h\delta_h^+}{\partial t}, \tag{3.2}$$

$$\int_0^{r_0}\frac{\partial\rho}{\partial t}r\,dr+\frac{\partial}{\partial x}\left\{\rho_0 w_0\frac{r_0^2}{2}\left(1-2\frac{\delta^+}{r_0}\right)\right\}=0. \tag{3.3}$$

The integration of the system (3.1)-(3.3) depends on the initial conditions. In view of their diversity, a particular case will be considered in which the flow rate of the incompressible fluid is nonstationary.

In this case the system (3.1)-(3.3) reduces to the differential equation

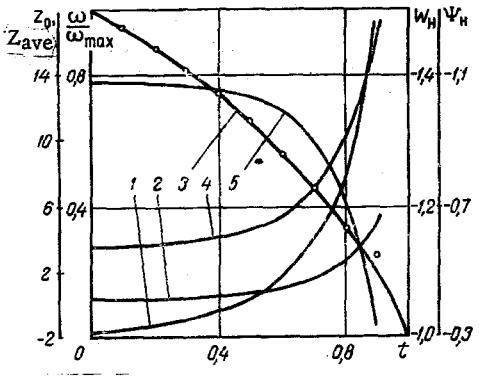

Fig. 5. Main flow parameters vs time at the boundary of the initial length. Curve 1) z_0 from (3.6); curve 2) z_{ave} from (3.6); curve 3) w/w_{max} from (3.12); curve 4) W_H from (3.4); curve 5) Ψ_H from (3.13). Dots) represent data from [7].

$$\frac{dX}{dW_0} = \frac{W_0 - W_0(W_0-1)\frac{1}{H}\frac{dH}{dW_0} + (1+H)(W_0-1)}{4HW_0^2\frac{c_f}{2} - H(W_0-1)\frac{D}{w_{01}^2}\frac{\partial w_{01}}{\partial t}}. \quad (3.4)$$

The integration of Eq. (3.4) can be carried out in several ways. The friction coefficients and the shape parameters which appear in the equation can be determined by using the methods described in §1 and 2 respectively. The gradient of the shape parameter can be computed from the equation

$$\frac{dH}{dW_0} = \frac{1}{\delta^{++}}\cdot\frac{d\delta^{++}}{dW_0} - \frac{H}{\delta^{++}}\cdot\frac{d\delta^{++}}{dW_0} \quad (3.5)$$

by inserting in it the gradients of the displacement thickness and of loss of the momenta obtained by differentiating suitable relations.

It is convenient to write the parameter characterizing the nonstationarity of the flow hydrodynamics in the form

$$z_0 = -\frac{2}{c_{f_0}}\cdot\frac{\delta}{r_0}\cdot\frac{1}{2}\left[\frac{D}{w_{01}}\cdot\frac{1}{W_0^2}\cdot\frac{dW_0}{dt} - \frac{1}{W_0}\cdot\frac{\partial}{\partial t}\left(\frac{D}{w_{01}}\right)\right]. \quad (3.6)$$

The thickness of the boundary layer is related to the parameters in a given section by

$$\frac{\delta}{r_0} = \frac{f_1}{2f_2} - \sqrt{\left(\frac{f_1}{2f_2}\right)^2 - \frac{\delta^+}{f_2 r_0}}, \quad (3.7)$$

$$f_1 = \frac{1}{\varkappa}\sqrt{\frac{c_{f_0}}{2}}\left[\frac{1}{2}\sqrt{\frac{n_0}{2}}\left(\frac{2\Psi}{n_0}-1\right)\ln\sqrt{\left|\frac{B}{C}\right|} + \frac{1}{2}\sqrt{3(\Psi+n_0)} - \frac{\sqrt{\Psi}}{2}\right],$$

$$f_2 = \frac{1}{\varkappa}\sqrt{\frac{c_{f_0}}{2}}\left[-\frac{1}{8}\sqrt{\frac{n_0}{2}}\left(\frac{\Psi^2}{n_0^2}+\frac{\Psi}{n}-\frac{3}{4}\right)\ln\sqrt{\left|\frac{B}{C}\right|} - \frac{1}{8}\left(\frac{\Psi^2}{n_0^2}-3\frac{\Psi}{n_0}+\frac{5}{4}\right)\cdot\frac{\sqrt{3(\Psi+n_0)}-\sqrt{\Psi}}{1-\frac{2\Psi}{n_0}} + \frac{1}{4}\left(\frac{\Psi^2}{n_0^2}-\frac{\Psi}{n_0}+\frac{1}{4}\right)\frac{3\sqrt{3(\Psi+n_0)}-\sqrt{\Psi}}{\left(1-\frac{2\Psi}{n_2}\right)^2}. \quad (3.8)$$

The relation between the velocity and the number R^{++} is found from Eq. (3.3) which in our case it is convenient to write as

$$4HR^{++} = R_1(W_0 - 1). \quad (3.9)$$

The law of friction under standard conditions is obtained from (1.13) and one has

$$\frac{c_{f_0}}{2} = \left(\frac{1-\omega_{10}}{\frac{1}{\varkappa}\ln\xi_{10}}\right)^2. \quad (3.10)$$

Thus the system of equations (3.1)-(3.10) is completely determined by the evolution of the turbulent boundary layer in isothermic conditions and by the appearance of nonstationarity. In the case of flux in the initial length of pipe its solution can be obtained by employing the following scheme.

1. From the given initial conditions $w_{01}/D = f(t)$ one can determine the value of velocity and of its derivative at the entry to the pipeline which corresponds to a given time instant and one evaluates the thickness of the boundary layer, the displacements and momenta.

2. Using the formula

$$\frac{dW_0^2}{dt} = \frac{4W_0\frac{c_f}{2} + (W_0-1)\frac{\partial}{\partial t}\left(\frac{D}{w_{01}}\right)}{D/w_{01}} \quad (3.11)$$

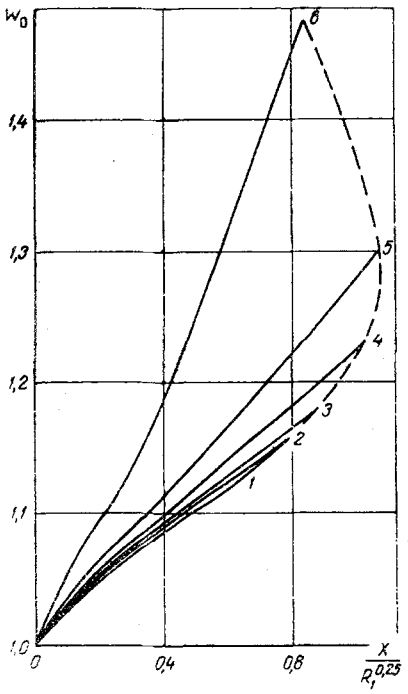

Fig. 6. Mean velocity curves: curve 1) t = 0; curve 2) 0.5; curve 3) 0.6; curve 4) 0.7; curve 5) 0.8; curve 6) 0.9. Computation of curves carried out by using (3.4).

one calculates the time-derivative of the velocity and the formula (3.6) yields the parameter n_0 in a section which corresponds to the integration step of Eq. (3.4).

3. Knowing the parameter n_0 one finds now ξ_1, ω_1 and Ψ by solving the system of equations (1.14), (1.18), and (1.19).

4. The thickness of displacements and the losses of momenta, of the boundary layer and the number R^{++} are now calculated.

The obtained values are used as the initial conditions in the next step.

Figures 5 and 6 show the results of the calculations using the above described method. The initial conditions from the experiments in [7] (Fig. 8b) were adopted as the starting data for the case of a slowed down flow. The average velocities in Fig. 6 shown by points were approximated by quadratic parabola to give time-dependent average velocity referred to its maximal value. The roughness of the pipeline was not taken into account. The time-variation of the basic flux parameters at the boundary of the initial length is shown in Fig. 5. The following special features are observed.

For small values of negative acceleration at the entry the flow on the conduit axis can be accelerated. This can be explained by the fact that complete acceleration in the potential core of the flow is a sum of the acceleration at the input and of the acceleration due to the growth of the displacement thickness. If the second contribution is considerable then negative values of the parameters z_0 and z_{ave} may be observed.

The modulus of acceleration increases with time, its contribution becomes greater and at some instant the parameters z_0 and z_{ave} assume positive values.

From this time instant the total flow decelerates. The way in which the nonstationarity parameter changes implies a specific law for variation of the relative friction coefficient Ψ. For accelerated flows it exceeds unity, for decelerated ones it is less than one. The average relative friction coefficient over a period is 0.7 which is in agreement with the experimental data of the authors of [7] (Fig. 7). As mentioned previously, a negative velocity gradient has a considerable effect on the integral characteristics of a turbulent boundary layer, in particular giving rise to the growth of the displacement thickness. This is indirectly confirmed by considerable velocity change of the initial length at the boundary as well as by calculations of velocity on the pipe axis along its length as shown in Fig. 6. The flow in the potential core was accelerated up to 0.5 sec since the acceleration due to the growth of displacement thickness prevailed over the initial deceleration. The curves 1 and 2 are very close to one another.

For large decelerations the displacement thickness changes considerably and the growth of relative velocity on the axis is appreciable.

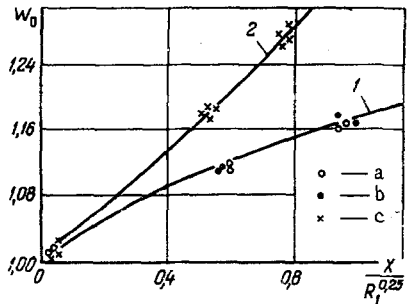

Fig. 7. W_0 vs $X/R_1^{0.25}$, a) $\partial(D/w_{01})/\partial t = 0$; b) 0.0028; c) 0.115. Curves obtained by employing (3.4); the points represent experimental results.

From Fig. 6 one can draw yet another important conclusion. The negative velocity gradient has a substantial effect on the growth of thickness of the boundary layer which manifests itself by the dependence of the length of the initial portion on time.

In view of the lack of experimental data on kinematic flow characteristics in the initial length of the pipe under given conditions an experimental investigation had to be carried out. Its first part includes the measurement of the total pressure in the premix chamber and of static pressure in the pipe length. It is our aim at this stage to determine the velocity in the flux potential core in the presence of nonstationarity.

The experimental set up consists of a closed-type flowing water hydrodynamic system. The following are its main elements: a water-supply system, pulsator with a premix chamber, experimental portion, automatic registration system of the parameters.

The supply system contains a pump TsV4/85, a buffer and a damper capacity.

To ensure a specified velocity law and its profile at the entry to the experimental portion a pulsator and a premix chamber are used.

The experimental portion is a seamless pipe made from stainless steel its internal diameter being 20 mm and its length 2200 mm. At the sections $x/2r_0 = 0.5$; 8; 12; 20 holes of $\phi 2.2$ mm were drilled and pipe connections welded on for static-pressure measurement.

An automatic registration system for the parameters ensures that the sought quantities are registered in less than $1/10^{th}$ of the measurement period. The system consists of DDV pressure transducers, KN-2M converters and of an N-700 oscillograph.

The inertia characteristics of the system fluid-transducers were estimated in accordance with [8].

Prior to starting the main experiments the sizing and calibration of the equipment was carried out. The sizing consisted in determining the reasons for hydrodynamic instability and flow pulsation. It was found that the presence of bends and turnings in the installations was the main source of pulsations. The hydraulic route was, therefore, completed using the smallest possible number of turnings. A partial suppressing of pulsations is achieved by damping capacity.

Calibration includes the checking of readings of all pressure measurements and of the secondary apparatus.

The main experiments refer to flows with decelerated as well as accelerated state of flux at the entry to the experimental portion. The experiments embrace the range of velocity from 0 to 6 m/sec and of acceleration from 0 to 50 m/sec. The Reynolds numbers corresponding to the velocities at the entry vary from $5.5 \cdot 10^4$ to $11.5 \cdot 10^4$.

The complete and static pressure measured during the experiment is used to find the velocity. It can be determined by solving the Lagrange—Cauchy equation,

$$\rho_0 \frac{\partial w_0}{\partial t} + \rho_0 w_0 \frac{\partial w_0}{\partial x} = -\frac{\partial}{\partial x}(P^+ - P). \tag{3.12}$$

In Fig. 7 these calculations are represented as functions

$$\frac{w_0}{w_{01}} = f\left(\frac{X}{R_1^{0.25}} t\right), \tag{3.13}$$

One observes the effect of the negative initial acceleration on the velocity change in the potential core. The effect of positive acceleration is negligible and was not noticeable in the experiments.

LITERATURE CITED

1. S. S. Kutateladze and A. N. Leont'ev, Turbulent Boundary Layer of Compressible Gas, Izd. SO AN SSSR, Novosibirsk (1962).
2. É. K. Kalinin and G. A. Dreitser, General and Theoretical Problems of Thermal Energy, Moscow (1969).

3. S. S. Kutateladze (editor), Heat-Mass Transfer and Friction in Boundary Layer, Izd. SO AN SSSR, Novosibirsk (1964).
4. I. V. Ginzburg, Aerodynamics, Vysshaya Shkola, Moscow (1966).
5. R. E. Gohnk and T. G. Hauratty, Chem. Eng. Science, 17, 867 (1962).
6. A. I. Leont'ev, B. P. Mironov, and A. V. Fafurin, PMTF, 1 (1967).
7. I. W. Daily, W. I. Hankey, R. W. Olive, and S. M. Gordaan, Trans. ASME, 76, No. 5 (1956).
8. A. N. Petunin, Methods and Technology of Parameter Measurements of Gas Flow, Mashinostroenie, Moscow (1972).